Article

Low-Field Magnetic Stimulation Alleviates MPTP Intoxicated Alterations on Motor Function and Dopaminergic Neurons in Male Mice

Sathiya Sekar[1#], Yanbo Zhang[2,‡,#], Hajar Miranzadeh Mahabadi[1], Benson Buettner[1] and Changiz Taghibiglou[1,*]

[1] Department of Pharmacology, College of Medicine, University of Saskatchewan, 107 Wiggins Road, Saskatoon SK, S7N 5E5, Canada

[2] Department of Psychiatry, 103 Hospital Drive, Royal University Hospital, Saskatoon, SK S7N 0W8, Canada

* Correspondence: changiz.taghibiglou@usask.ca; Phone: +1-306-966-8816

#- Equal contribution.

‡-Present Address: Psychiatry Department, Faculty of Medicine & Dentistry, University of Alberta, Edmonton, AB, Canada T6G 2R7

Abstract: Recent studies show that repetitive transcranial magnetic stimulation (rTMS) improves cognitive and motor functions in patients with Parkinson's Disease (PD). Gamma rhythm low-field magnetic stimulation (LFMS) is a new non-invasive rTMS technique that generates diffused and low-intensity magnetic stimulation to deep cortical and subcortical areas. To investigate potential therapeutic effects of LFMS in PD, we subjected an experimental mouse model to LFMS (as early treatment). We examined the LFMS effect on motor functions as well as neuronal and glial activities in 1-methyl-4-phenyl-1,2,3,6-tetrahydropyridine (MPTP) induced male C57BL/6J mice. Mice received MPTP injection (30 mg/kg, i.p., once daily for 5 days) followed by LFMS treatment, 20 minutes each day for 7 days. LFMS treatment improved motor functions compared to the sham-treated MPTP mice. Further, LFMS significantly improved tyrosine hydroxylase (TH) and decreased glial fibrillary acidic protein (GFAP) levels, in substantia nigra pars compacta (SNpc) and non-significantly in striatal (ST) regions. LFMS treatment improved neuronal nuclei (NeuN) level in SNpc. Our findings suggest that early LFMS treatment improved the neuron survival and in turn, motor functions in MPTP intoxicated mice brain. Further investigation is required to clearly define the molecular mechanisms by which LFMS improves motor and cognitive function in PD patients.

Keywords: MPTP; LFMS; neurons-glial functions; motor function; Parkinson's disease

1. Introduction

Parkinson's disease (PD) is a progressive neurodegenerative disorder affecting approximately 1% of the population over the age of 60 worldwide [1]. PD is clinically characterized by slow or decreased movement, resting tremor, postural instability and various other symptoms. It is primarily caused by the degeneration of dopaminergic neurons in substantia nigra pars compacta (SNpc) and depletion of dopamine in striatum (ST) [2-5]. Depletion of dopamine and dysregulation of dopamine receptors result in the disruption of circadian rhythms in PD [6]. Unfortunately, current approved treatments of PD decrease the symptoms but do not halt the disease progression. Most of the developed medications, for rescuing dopaminergic neurons and restoring motor and non-motor functions, have failed in clinical trials because of low efficacy or adverse effects [7]. As such, novel therapeutic strategies that prevent disease progression are urgently needed.

Repetitive transcranial magnetic stimulation (rTMS) is a non-invasive neurostimulation technique that is widely used as a tool for studying brain function and treating brain disorders such as major depression, PD and Alzheimer's disease [8-10]. rTMS generates brief and intense pulses of

 doi:10.20944/preprints202305.0214.v1

magnetic stimulation (peak magnetic field is around 1–2 Tesla, generating electric fields, E≥100 V/m) to depolarize underlying neurons in focal brain areas [8]. A recent meta-analysis revealed that high frequency-rTMS (HF-rTMS) (≥5Hz) treatment in bilateral motor cortex (M1) improved both upper limb and walking performances in PD [9]. This finding was recommended as a treatment guideline for PD by a European expert consensus [11]. The same guideline also suggests that rTMS involving larger cortex area and more sessions may further enhance treatment efficacy. In addition to motor function, the effect of rTMS in treating depression and cognitive deficits in PD has been studied [12]. The dorsolateral prefrontal cortex (DLPFC) is the most studied brain area for depression and cognitive deficit in PD. The evidence to support the efficacy of rTMS treatment for cognitive deficits reamins conflicting [12, 13]. Inconsistent results in support of rTMS is likely due to differences in treatment location as well as strength and duration of stimulation protocols [14]. In addition to rTMS, a few studies have explored the therapeutic potential of transcranial pulse electromagnetic field (T-PEMF) and transcranial direct current stimulation (tDCS) in PD [15, 16]. Distinguished from conventional rTMS, T-PEMF and tDCS generate a low electromagnetic field below the action potential threshold [17]. Although these techniques have shown promising results, further studies are warranted to determine their true clinical impact on patients with PD.

Low-field magnetic stimulation (LFMS), a new rTMS technology that produces low-intensity magnetic stimuli [10-50 Gauss (0.001-0.005 Tesla)], has shown rapid mood-elevating effects in patients with major depressive disorder (MDD) and bipolar disorder [18-20]. Importantly, LFMS produces diffuse magnetic stimulation with intermittent gamma bursts in cortical regions without the risk of inducing seizure or other side effects often seen in rTMS treatement, such as painful scalp sensations and headache [19-24]. In addition, LFMS treatment does not require hospitalization and patients can be treated anywhere. The intensity of magnetic stimulation with LFMS is also very low in comparison to rTMS (1-2 Telsa) technology and may therefore reduce the risk of side effects. In preclinical models of disease, LFMS treatment has been shown to be neuroprotective [25, 26]. Our previous work with LFMS in a mouse model of traumatic brain injusry (TBI) also showed promising results, with LFMS treatment recovering motor and cognitive functions associated with brain injury [27]. In cuprizone models of Multiple Sclerosis, LFMS has also been shown to promote myelin repair [28, 29]. We therefore hypothesize that LFMS may improve motor functions and possess neuroprotective effects, supporting its use as a treatment strategy for patients with PD. In the present study, we examined the effect of LFMS on motor deficits and neuronal degeneration in 1-methyl-4-phenyl-1,2,3,6-tetrahydropyridine (MPTP)-intoxicated sub-chronic mouse model of PD. In addition, we studied the effect of LFMS on MPTP induced astroglial and microglial activation in SNpc and ST regions.

2. Results

2.1. LFMS treatment improved motor function in MPTP intoxicated mice.

Motor function tests were performed for all the experimental mice. Beam walk and rotarod tests were studied 48h after the last MPTP injection, and open field locomotor and stride length were measured, on the next day. The values obtained from each test were collected and the difference between the groups were analyzed using one-way ANOVA followed by tukey's multiple comparison as post hoc. Statistical results showing the impact of LFMS treatment on the motor function of MPTP intoxicated mice are summarized in the next four sections.

2.1.1. Beam walk test

Beam walk test was performed for all the experimental mice to asses the motor coordination. The mice were pre-trained for beam walk and then assessed, 48 h after the last MPTP injection. MPTP mice took longer time to traverse the narrow beam and their immobility period was increased, compared to the normal control mice ($P< 0.001$ and 0.01, respectively). Both the time taken to transverse the beam and the immobility period dropped significantly after LFMS treatment of MPTP mice ($P< 0.001$ and 0.01, respectively). LFMS alone treatment showed no significant change in the

 doi:10.20944/preprints202305.0214.v1

time taken and the immobility period compared to the normal control group (P= 0.989 and 0.999, respectively). The one-way ANOVA revealed a significant difference between the groups [time taken: $F(3, 46)= 10.06$; n=12 for GI and GIV, and 13 for GII and GIII; $P<0.001$ and immobility period: $F(3, 46)= 6.489$; n=12 for GI and GIV, and 13 for GII and GIII; $P<0.001$] **(Fig. 2A and 2B)**.

Preprints (www.preprints.org) | NOT PEER-REVIEWED | Posted: 4 May 2023 doi:10.20944/preprints202305.0214.v1

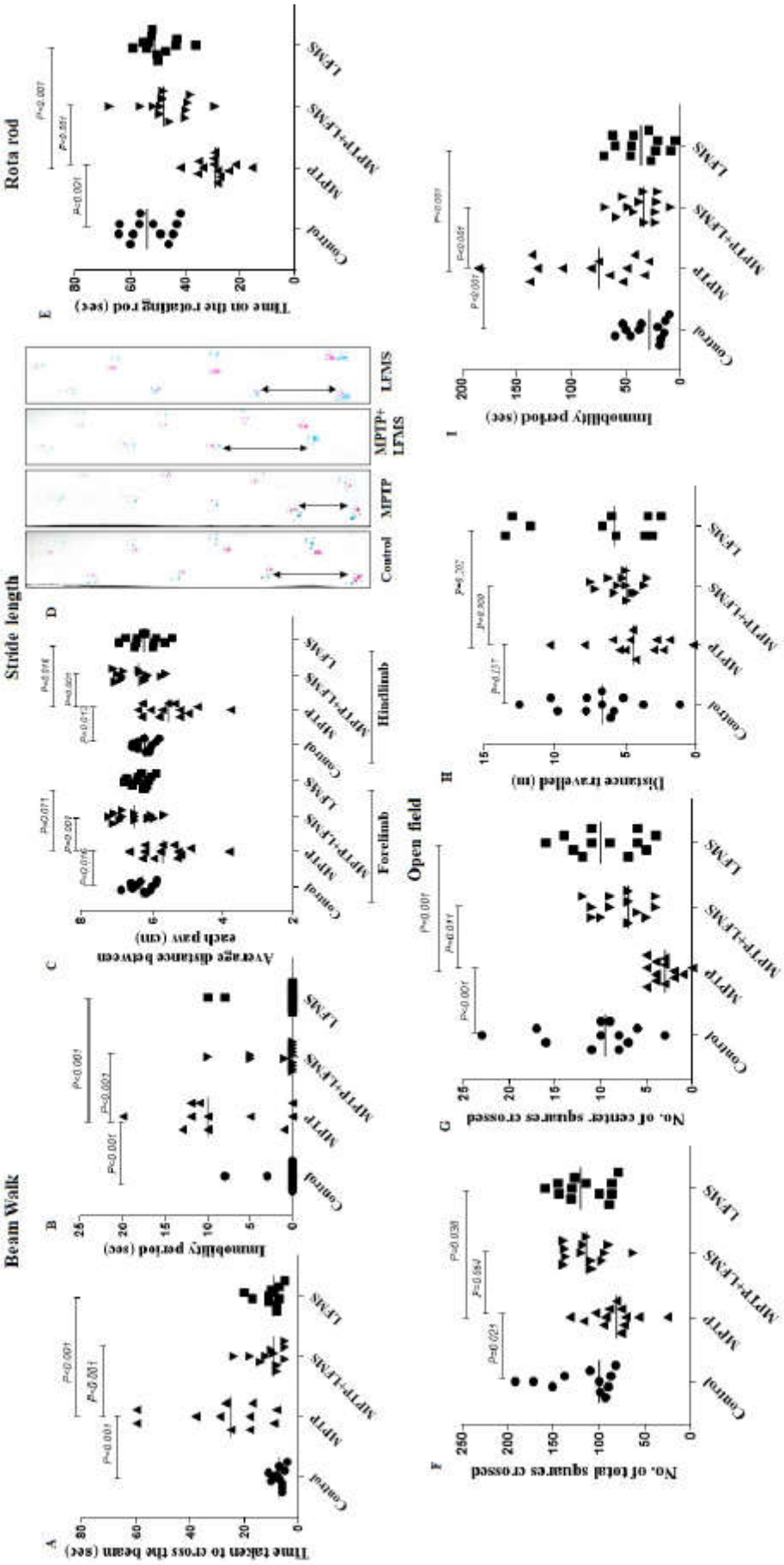

Figure 2. Effect of LFMS on functional outcome in MPTP mice. (A & B) graphs represents the time taken to cross the beam (s) and immobility period (s), respectively in beam walk test; (C) graph

 doi:10.20944/preprints202305.0214.v1

represents the average distance between the two successive fore or hind paws (average of three readings) in gait test; (D) representative images of the foot paws of (1) control, (2) MPTP, (3) MPTP+LFMS and (4) LFMS mice in gait test; (E) graph represents the time on the rotating rod (s) using rotarod test; (F-I) graphs representing the total number of squares crossed, number of center squares crossed, total distance travelled and immobility period, respectively in open field test; n=12 for control and LFMS groups and 13 for MPTP and MPTP+LFMS groups.

2.1.2. Stride length

In addition to beam walk, stride length test was also carried out for all the experimental mice to assess the motor coordination. The average distance between the two successive forelimb and hindlimb foorprints were measured. The average distance between the two successive limbs was significantly reduced in the MPTP mice compared to the normal control mice (P= 0.005 and 0.006, respectively), whilst the average distance was restored with the LFMS treatment (P< 0.001). The values obtained from LFMS alone treated mice were found to be not significantly different with that of the normal control mice (P= 0.999). The one-way ANOVA results showed significant difference between the groups [Forelimb: F(3, 46)= 9.241; n=12 for GI and GIVand 13 for GII and GIII; P<0.001; hindlimb: F(3, 46)= 8.707; n=12 for GI and GIVand 13 for GII and GIII; P<0.001]. **(Fig. 2C and 2D)**

2.1.3. Rotarod Test

Rotarod test was performed 48 h after the last MPTP injection. Mice were allowed to walk on the rotating rod with an accelerated rotation rate of 4 rpm/s and the time taken by the mice on the rotating rod was recorded. MPTP mice were not able to walk on the rotating rod and fell within a short span of time (P<0.001), whilst LFMS treatment in MPTP mice significantly improved (P<0.001) the time taken to walk, indicating a restoration effect. Mice treated with LFMS alone performed similar to that of control mice (P=0.720). The one-way ANOVA showed a significant difference between the groups [F(3, 46)= 23.680; n=12 for GI and GIVand 13 for GII and GIII; P<0.001]. **(Fig. 2E)**

2.1.4. Open field locomotor activity

Open field exploration showed that MPTP mice had reduced the mobility during 5 min observation as evidenced by the decreased total number of squares crossed, and the number of center squares crossed, in comparison to the normal control mice (P= 0.021, and P<0.001, respectively), whereas the reduction in total distance travelled did not reach to a significant level (P= 0.151) . A significant increase in immobility period was also observed (P<0.001). MPTP mice treated with LFMS resulted in a non- significant (P= 0.064) increase in total number of squares crossed **(Fig. 2F)**, and significant (P= 0.011) increase in center squares crossed **(Fig. 2G**). While the effect of LFMS treatment on the distance travelled by intoxicated mice **(Fig. 2H)** was not significant (P= 0.898), it significantly decreased immobility period **(Fig. 2I**), compared to the MPTP mice (P<0.001). The values obtained in LFMS alone treated mice were found to be comparable to that of control mice (P= 0.990, 0.863, 0.983 and 0.976, respectively). The one-way ANOVA analysis showed that except with the distance travelled [F(3, 46)= 1.972; n=12 for GI and GIVand 13 for GII and GIII; P=0.13], there were significant differences between the treatment groups [total number of squares crossed: F(3, 46)= 3.819; n=12 for GI and GIVand 13 for GII and GIII; P=0.013, center squares crossed: F(3, 46)= 10.270; n=12 for GI and GIVand 13 for GII and GIII; P<0.001, and immobility period: F(3, 46)= 9.810; n=12 for GI and GIVand 13 for GII and GIII; P<0.001].

2.2. LFMS treatment significantly improved TH and NeuN levels in SNpc and ST regions of MPTP intoxicated mouse brain.

Immunohistochemistry of TH immune positive cells in SNpc **(Fig. 3A-3D)**, intensity of immunopositivity in ST **(Fig. 3F-3I)** and NeuN immunopositive cells in SNpc **(Fig. 4A-4D)** and ST **(Fig. 4E-4H)** regions were measured. The difference between the groups were analyzed using two-way ANOVA. A significant decrease in percentage of TH and NeuN immunopositivity in SNpc (P<0.001) and ST (P<0.001 and P= 0.025, respectively) regions of MPTP mouse brain were observed,

Preprints (www.preprints.org) | NOT PEER-REVIEWED | Posted: 4 May 2023 doi:10.20944/preprints202305.0214.v1

compared to the control mouse brain. LFMS treatment restored these alterations significantly in SNpc **(Fig. 3E and 4I)** region, by increasing TH and NeuN immunostaining compared to MPTP mouse brain (P= 0.007 and 0.003, respectively), whilst no significant difference was observed in ST **(Fig. 3J and 4I)** region (P= 0.254 and 0.828, respectively). LFMS alone treatment showed similar morphology to that of normal mice (P= 0.990). The two-way ANOVA between the groups showed a significant differences for TH and NeuN [TH: $F(3, 40) = 45.55$; n=6; $P<0.001$, NeuN: $F(3, 40) = 16.57$; n=6; $P<0.001$], whereas the interaction between SNpc and ST were not significant [TH: $F(3, 40) = 0.680$; n=6; P= 0.570 and NeuN: $F(3, 40) = 2.247$; n=6; P=0.098]**.**

Preprints (www.preprints.org) | NOT PEER-REVIEWED | Posted: 4 May 2023 doi:10.20944/preprints202305.0214.v1

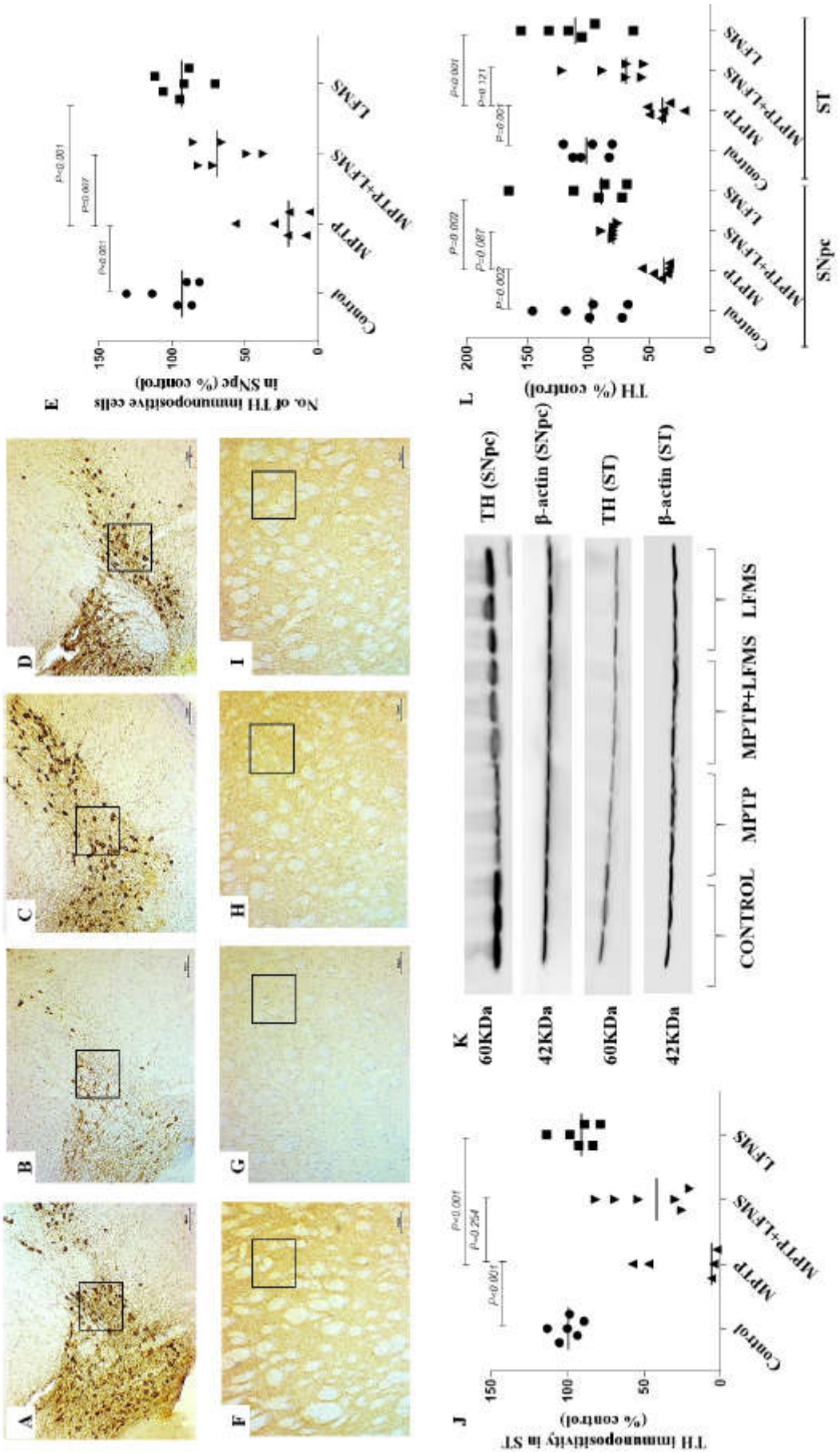

Figure 3. Effect of LFMS on tyrosine hydroxylase (TH) level in SNpc and ST regions of MPTP mice brain. Representative images of TH immunopositive cells in SNpc (A-D; at 4x magnification) and ST

 doi:10.20944/preprints202305.0214.v1

(F-I; at 10x magnification) regions of control (A and F), MPTP (B and G), MPTP + LFMS (C and H) and LFMS alone (D and I) treated mice brain; box represented on the images are the region where quantification was performed; (E) graph representing the percentage number of TH immunopositive cells in SNpc region and (J) TH immunopositivity in ST region. (K) Representative western blot images of TH level and their respective loading control in SNpc and ST regions of control, MPTP, MPTP+LFMS and LFMS mice brain, (L) graph representing its % TH level with that of control by western blotting, n=6.

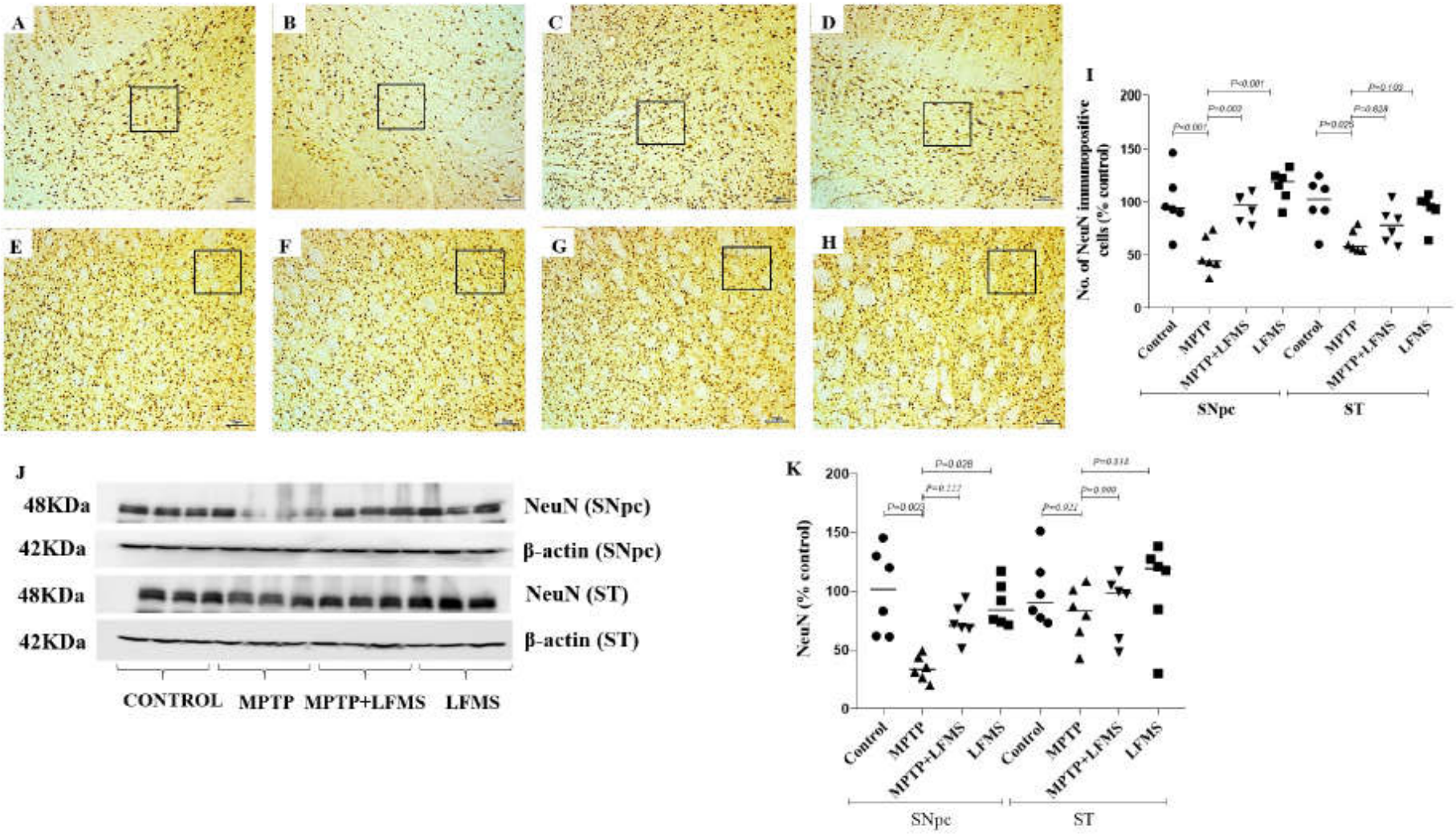

doi:10.20944/preprints202305.0214.v1

 doi:10.20944/preprints202305.0214.v1

Figure 4. Effect of LFMS on Neuronal nuclei (NeuN) level in SNpc and ST regions of MPTP induced mice. Representative images of NeuN immunopositive cells in SNpc (A-D; at 4x magnification) and ST (E-H; at 10x magnification) regions of control (A and E), MPTP (B and F), MPTP + LFMS (C and G) and LFMS alone (D and H) treated mice brain; box represented on the images are the region where quantification was performed; (I) graph representing the percentage number of NeuN immunopositive cells in SNpc and ST regions. (J) Representative western blot images of NeuN level and their respective loading control in SNpc and ST regions of control, MPTP, MPTP+LFMS and LFMS mice brain, (K) Graph representing the levels of NeuN level by western blotting, n=6.

Western blotting in SNpc and ST regions between the groups were represented in **Fig. 3K and 4J** and the difference between the groups were analyzed using two-way ANOVA. MPTP mice showed a significant decrease in TH and NeuN levels (P=0.002 and 0.003 for SNpc, 0.001 and 0.921 for ST regions, respectively), compared to the normal control mouse brain. A non-significant increase in TH **(Fig. 3L**), and NeuN **(Fig. 4K**) levels were observed in LFMS treatment compared to the MPTP mouse brain (P=0.087 and 0.222 for SNpc, 0.121 and 0.999 for ST regions, respectively). The values obtained in the LFMS alone treatment were comparable to that of normal control mice (P=0.990). The two-way ANOVA between the groups showed a significant difference [TH: F (3,40) = 19.66; n=6; P<0.001, NeuN: F (3,40) = 6.114; n=6; P=0.002]. The interaction between SNpc and ST regions was found to be non-significant [TH: F (3, 40) = 0.283; n=6; P=0.837 and NeuN: F (3, 40) = 1.617; n=6; P=0.201]**.**

2.3. LFMS treatment reduced GFAP level, thereby suppress gliosis in MPTP intoxicated mouse brain.

Immunohistochemistry of GFAP immunopositive cells in SNpc and ST regions were represented in **Fig. 5A-5D** and **Fig. 5E-5H**, respectively. The difference between the groups were analyzed using two-way ANOVA. Measuring GFAP immunopositive cells showed a significant increase in GFAP positive cells in SNpc and ST regions (P=0.001 and P<0.001, respectively), respectively of MPTP mice compared to the control mouse brain. LFMS treatment significantly reduced these alterations in SNpc region (P=0.013), whilst non-significant differences were observed in ST region (P=0.192), compared to the MPTP mice brain (**Fig. 5I**). LFMS alone treated mouse brains showed similar morphology compared to normal mice (P=0.999). The two-way ANOVA analysis between the groups was found to be significant [F (3, 40) = 81.89; n=6; P<0.001, interaction between SNpc and ST: F (3, 40) = 34.08; n=6; P<0.001]**.**

Preprints (www.preprints.org) | NOT PEER-REVIEWED | Posted: 4 May 2023 doi:10.20944/preprints202305.0214.v1

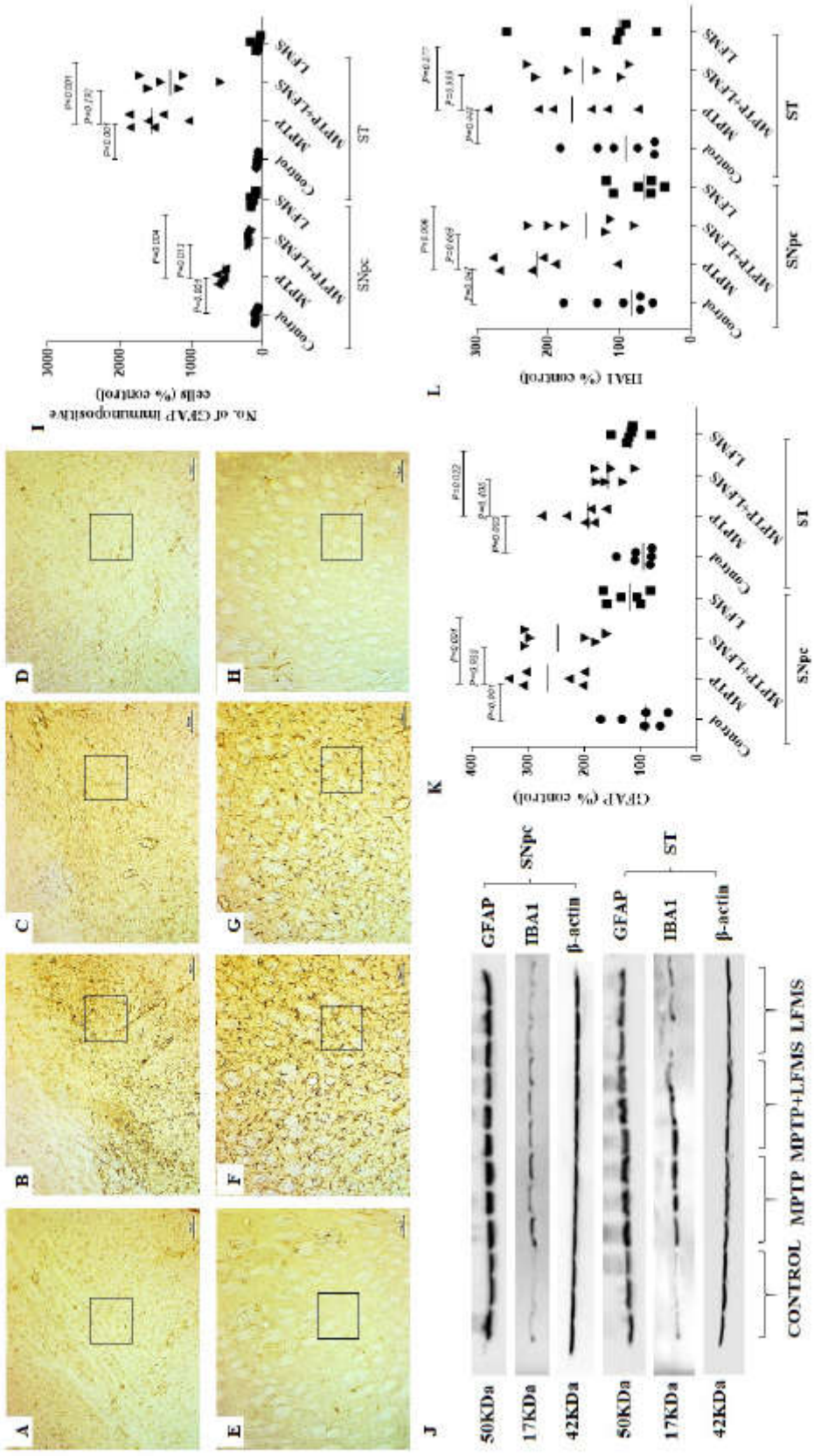

Figure 5. Effect of LFMS on glial fibrillary acidic protein (GFAP) level in SNpc and ST regions of MPTP induced mice. Representative images of GFAP immunopositive cells in SNpc (A-D) and ST (E-H) regions (at x 40 and 100 magnification, respectively) of control (A and E), MPTP (B and F), MPTP + LFMS (C and G) and LFMS alone (D and H) treated mice brain; box represented on the images are

 doi:10.20944/preprints202305.0214.v1

the region where quantification was performed; (I) graph representing the percentage number of GFAP immunopositive cells in SNpc and ST regions. (J) Representative western blot images of GFAP and IBA1 levels and their respective loading control in SNpc and ST regions of control, MPTP, MPTP+LFMS and LFMS mice brain, Graph represents the levels of GFAP (K) and IBA1 (L) levels by western blotting, n=6.

Effect of LFMS on astroglial (GFAP) and microglial (IBA1) markers in SNpc and ST regions of MPTP induced mouse brain were measured using western blotting (Representative images in **Fig. 5J**) and the difference between the groups were analyzed using two-way ANOVA. MPTP mice showed significant increase in GFAP (P<0.001 and P=0.003, in SNpc and ST, respectively) and while IBA1 levels increased significantly in SNpc (P= 0.041), the alteration in ST was non-significant (P= 0.448) compared to the normal control mouse brain. The effect of LFMS treatment on GFAP (**Fig. 5K;** P=0.998 and 0.408, respectively) and IBA1 (**Fig. 5L;** P=0.633 and 0.999, respectively) levels were not significant, compared to the MPTP mouse brain. LFMS alone treatment showed no difference in comparison to the normal control mice (P=0.990). The two-way ANOVA analysis between the groups was found to be significant [GFAP: F (3, 40) = 25.29; n=6; P<0.001 and IBA1: F (3, 40) = 6.855; n=6; P=0.001]. The interaction between SNpc and ST regions was not significant [GFAP: F (3, 40) = 2.822; n=6; P=0.051 and IBA1: F (3, 40) = 1.193; n=6; P=0.325]**.**

2.4. Effect of LFMS treatment on caspase-3 activation in SNpc and ST regions of MPTP induced mouse brain.

Western blot images of total and cleaved caspase 3 were represented in **Fig. 6A** and the difference between the groups were analyzed using two-way ANOVA **(Fig. 6B).** A significant increase in cleaved to total caspase-3 ratio was observed in SNpc and ST (P<0.001 and P=0.01, respectively) regions, respectively of MPTP mouse compared to normal control mouse brain. While LFMS treatment decreased caspase-3 ratio, non-significantly in SNpc (P=0.055) and it had no significant effct in ST regions (P= 0.187). LFMS alone treatment showed no such differences with that of normal mice brains (P=0.999). The two-way ANOVA analysis was performed for the cleaved to total caspase 3 ration and F value between the groups was found to be F (3, 40) = 17.08; n=6; P<0.001 and the interaction between SNpc vs ST regions was F (3, 40) = 0.376; n=6; P=0.771**.**

Preprints (www.preprints.org) | NOT PEER-REVIEWED | Posted: 4 May 2023 doi:10.20944/preprints202305.0214.v1

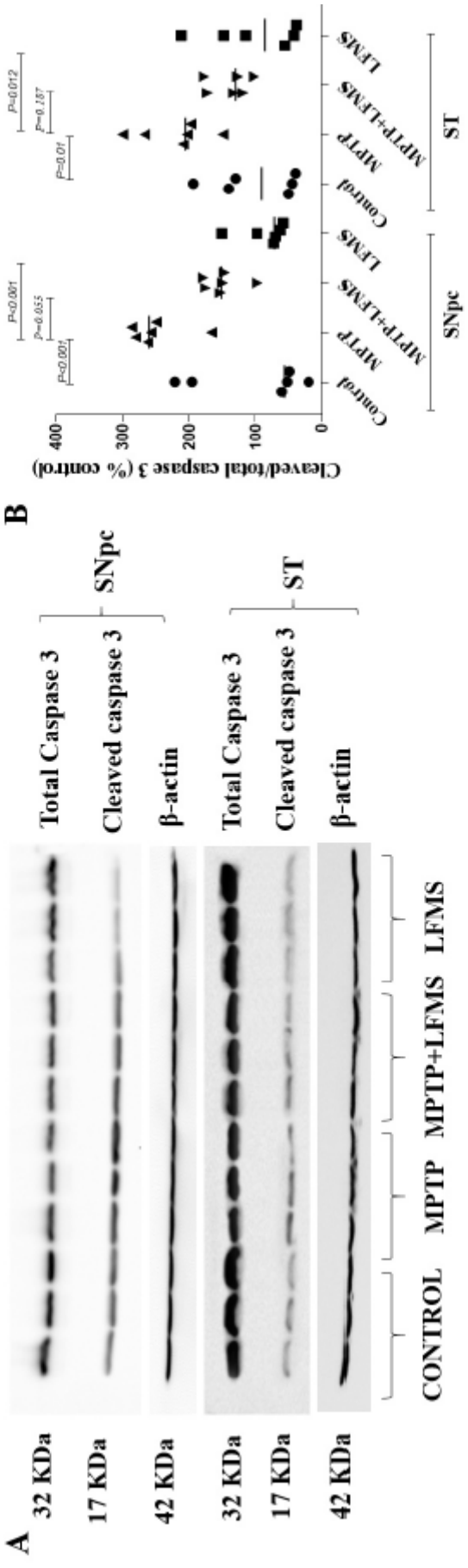

Figure 6. Effect of LFMS on caspase-3 level using western blot analysis in SNpc and ST regions of MPTP induced mice brain. (A) Representative western blot images of cleaved and total caspase-3

Preprints (www.preprints.org) | NOT PEER-REVIEWED | Posted: 4 May 2023 doi:10.20944/preprints202305.0214.v1

levels and their respective loading control in SNpc and ST regions of control, MPTP, MPTP+LFMS and LFMS mice brain, respectively; (B) graph represents the ratio of cleaved to total caspase-3; n=6.

2.5. Effect of LFMS treatment on dopamine level in ST region of MPTP mouse brain.

Dopamine level in ST regions of the experimental mouse brain was analyzed using ELISA technique and the difference between the groups were analyzed using one-way ANOVA. The Dopamine level reduction in the MPTP mouse brain was not significant when compared with that the control brains (*P*=0.490). LFMS treatment appeared to increase the dopamine level in ST region in comparison to the MPTP intoxicated mouse brain, however, it did not reach to a significant level (*P*=0.089). LFMS alone treated brain was comparable with that of the normal control mouse brain (*P*=0.997). No significant difference between the groups were observed in the one-way ANOVA analysis [F(3, 16)= 2.189; n=5; *P*=0.129] **(Fig. 7).**

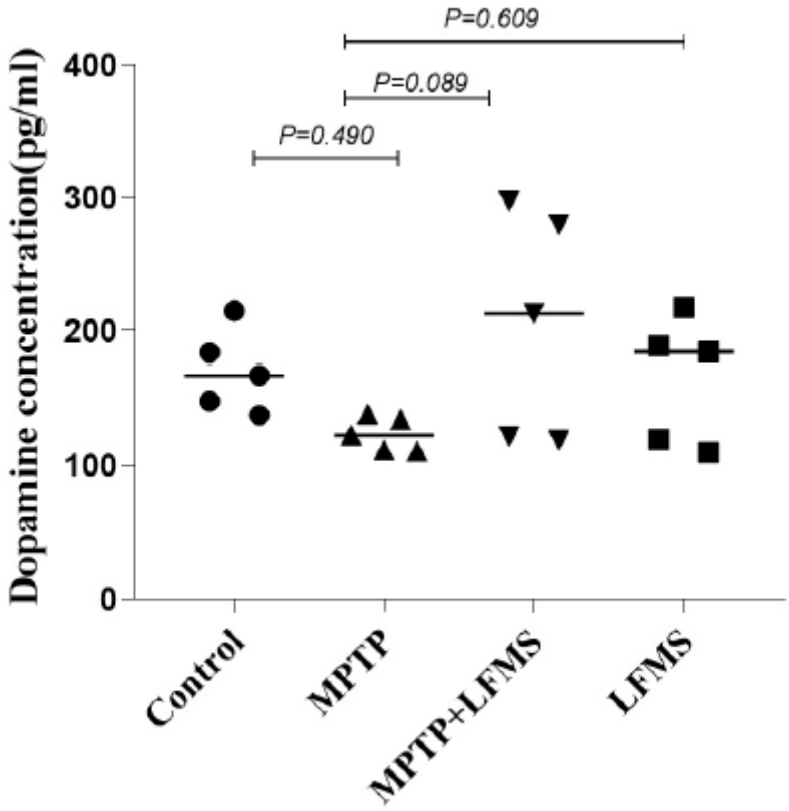

Figure 7. Effect of LFMS on striatal dopamine level using ELISA technique in MPTP induced mice brain. Graph represents the concentration of dopamine in ST regions of control, MPTP, MPTP+LFMS and LFMS mice brains, respectively; n=5.

3. Discussion

The present study was the first evidence to demonstrate the healing effect of LFMS on MPTP induced PD mouse model. LFMS treatment restores motor function in MPTP mice as evidenced by beam walk, stride length, rotarod and open field locomotor activity. Further, LFMS increased the TH level in SNpc region, which may contribute to dopaminergic neuronal protection/recovery. LFMS treatment reduced astrogliosis (GFAP) in MPTP-intoxicated mouse brain. Based on the above observations, we suggest that LFMS plays a significant role in restoring the dopaminergic functions, partly by regulating glial reactivity and motor functions in MPTP induced PD model and thus, it may be used as early therapeutic choice in the management of PD.

Evidences support that aberrant gamma oscillations have been linked to the neurological diseases and movement related changes of gamma amplitude was recorded in patients with

 doi:10.20944/preprints202305.0214.v1

neurological symptoms [30-32]. Researchers suggest that striatal gamma oscillation was decreased under low dopaminergic tone [33]. In the present study, the restorative effect of motor function in MPTP mice treated with LFMS may be due to the modulation of gamma synchronization in neurons. Neuronal alterations in PD are not restricted to only dopaminergic neurons, however the dopaminergic neurons in the nigrostriatal pathway degenerate to a greater extent than other neurons [34]. TH is the rate limiting enzyme in dopamine homeostasis and it has a direct link to PD pathogenesis [35-37]. Dong et al. [25] reported that low-frequency rTMS improved TH expression in an experimental mouse model of PD. In the present study, the observed increase in SNpc and ST TH level by western blotting and TH immunostaining in LFMS treatment are corroborated with the above finding. LFMS treatment also improved the dopamine level in ST region which suggests a potential neuroprotective effect of LFMS on dopaminergic neurons in MPTP intoxicated mouse model of PD. Furthermore, the decreased cleaved to total caspase-3 ratio in LFMS treatment also suggests the protective effect of LFMS against apoptotic pathway.

Astrocyte-neuronal interlink plays a vital role in central nervous system homeostasis. Activation of astrocytes has been associated with various neurodegenerative diseases including PD [31]. Increased expression of GFAP, a biomarker representing astrocyte activation and astrogliosis, has been extensively reported in cellular and experimental animal models of PD [38, 39]. In addition, microglia are activated during any neuronal insults. Neuroinflammation mediated by microglia is associated with the degeneration of dopaminergic neurons [40, 41]. Activation of microglia releases reactive oxygen species and cytokines, leading to the death of dopaminergic neurons [42]. In the present study, the decreased levels of GFAP and IBA1 in MPTP mice brain treated with LFMS suggest that LFMS restores neuronal function from astrogliosis and inflammatory insults. Immunohistochemical analysis showed that LFMS treatment decreased SNpc GFAP level compared to MPTP mice brain but the values were found to be non-significant in western blotting. The similar result was observed in the ST region and by increasing sample size may clearly define these differences. Reactive astrocytes have been reported to be involved in neurological recovery of stroke models [43]. Astrogliosis under certain circumstances may lead to harmful effects. The observed changes in GFAP level may be beneficial or harmful to the neuronal circuits. However, LFMS decreased reactive astrocytes and inflammation which may be beneficial in the management of PD.

Repetitive transcranial magnetic stimulation (rTMS) has been extensively studied for the possible treatment for PD. Various clinical studies suggested that rTMS plays a key modulatory role in restoring motor functions in PD [44-46]. Matsumoto and Ugawa [47] suggested that rTMS exerted beneficial effects on motor symptoms by inducing synaptic plasticity in PD patients [48]. The beneficial effects of rTMS are also attributed to neurotransmitter restoration and improved synaptic plasticity [49]. A single TMS treatment improved the mRNA levels of neurotrophic factors and prevented neuronal death by enhancing neurogenesis. Also, studies showed that 8-weeks treatment with T-PEMF improved motor function and neuronal recovery through neurotrophic factors and anti-inflammatory effects in PD patients but these treatments showed minimal effects and required other options [15, 51]. Recently, we showed that LFMS, which is a non-invasive, simple and laptop-like device, has promising results in the treatment of traumatic brain injury mouse model [27]. The results obtained in the present study clearly showed that LFMS treatment may be a beneficial treatment option for the management of PD. External magnetic field may provide an alternative to invasive brain surgeries and may help PD patients in a more convenient way.

In conclusion, LFMS decreased GFAP level and increased TH level in MPTP mice, indicating LFMS protects the dopaminergic neurons from MPTP insult. Additionally, LFMS improved motor function as evidenced from beam walk, rotarod, stride length and open field locomotor tests in the experimental mouse model of PD, through unknown mechanisms. The study was the first evidence to show the therapeutic effect of LFMS and we anticipate that this non-invasive and portable method of treatment may benefit the patients and provide a new insight in the management of PD, without the side effects reported with TMS treatment. In order to take the results from bench to bedside, further detailed investigation on restoring dopaminergic neurons in both the sex is warranted to clearly elucidate the exact cellular events using different experimental models of PD. Although LFMS stimulation showed promising results in the present study and was exposed to the whole body, the

 doi:10.20944/preprints202305.0214.v1

effect of LFMS on other parts of the body and their relations with brain neuronal restoration, if any, will be studied in detail in our future investigations. Further studies also warranted in elucidating the therapeutic effect of LFMS in PD treatment.

4. Materials and Methods

4.1. Chemicals and Reagents

MPTP was purchased from Sigma-Aldrich, Canada. Rabbit anti-tyrosine hydroxylase (TH; Cat# ab6211, RRID: AB_2240393) and mouse anti-neuronal nuclei (NeuN; Cat# MAB377, RRID: AB_2298772) were obtained from Abcam and Millipore, respectively; rabbit anti-ionized calcium-binding adapter molecule 1 (IBA1; Cat# MA5-36257, RRID: AB_2890455) and mouse anti-glial fibrillary acidic protein (GFAP; Cat# MA5-12023, RRID: AB_10984338) were purchased from Invitrogen; rabbit anti-caspase-3 (Cat# 9662S, RRID: AB_331439), goat anti-mouse IgG (HRP linked; Cat# 7076S, RRID: AB_330924) and goat anti-rabbit IgG (HRP linked; Cat# 7074S, RRID: AB_2099233) were from Cell Signaling; goat biotinylated anti-mouse IgG (H&L; Cat# BA-9200, RRID: AB_2336171), goat biotinylated anti-rabbit IgG (H&L; Cat# BA-1000, RRID: AB_2313606) and elite ABC-peroxidase kit (Cat# PK-6100, RRID: AB_2336819) were purchased from Vector Laboratories; mouse Anti-ß actin (C4) HRP (Cat# sc-47778 HRP, RRID: AB_2714189) was purchased from Santa Cruz Biotechnology; dopamine (DA) ELISA kit (Cat# RD-DA-Ge) was obtained from Reddot Biotech Inc. All other chemicals and reagents used were of analytical grade.

4.2. Animals

Ten-week-old male C57BL/6J mice (Charles River, Montreal, Canada; Cat # CRL: 027, RRID: IMSR_CRL:027) were used for the study. All the animals were housed in groups (2-5 animals/cage) under 12 h light and 12 h dark cycle with temperature control (~21°C) and were provided with standard food and water *ad libitum*. The experiment was approved by the University Animal Care Committee (UACC), University of Saskatchewan, Saskatoon SK, Canada, and performed following the Guidelines of the Canadian Council on Animal Care (CCAC).

4.3. Experiment design and treatment

Animals were acclimatized for 7 days to the laboratory conditions before experimentation. Following acclimatization, animals were pre-trained for beam walk test until ceiling performance was reached. The animals were then randomly assigned to one of the following groups (12-13 mice/ group): GI – control (n=12), GII – MPTP (n=13), GIII - MPTP + LFMS (n=13) and GIV – LFMS (n=12).

MPTP was administered to group II and III, intraperitoneally (i.p.) at 30 mg/kg, once daily for 5 days. This sub-chronic dose regimen was selected as they induce the depletion of 90% of TH proteins and increase astrogliosis at 24 h after injection [51]. Normal saline (NS, 0.9% NaCl) was administered i.p., once daily for 5 days to the control and LFMS groups. LFMS treatment was provided to the respective animals for a period of 20 min, 4 h after first MPTP or NS injection and then once daily for 6 days. Sham treatment was given to the control and MPTP groups by placing them on the machine for 20 min without any magnetic stimulation. The LFMS device (Beijing Antis Biotech Co., Ltd.) generates time-varying magnetic stimulation every 2 sec, followed by an 8-sec resting interval. The magnetic field changed every 2 min between the uniform and linear gradient. Each 2-sec stimulation consists of 80 trains spiking 6 msec at intervals of 19 msec, which constitute the intermittent gamma burst stimulation at 40 Hz. The magnetic flux density was composed of six pulses with 0.13 msec width and 1000 Hz frequency as described previously [52, 53] **(Fig. 1)**.

Preprints (www.preprints.org) | NOT PEER-REVIEWED | Posted: 4 May 2023 doi:10.20944/preprints202305.0214.v1

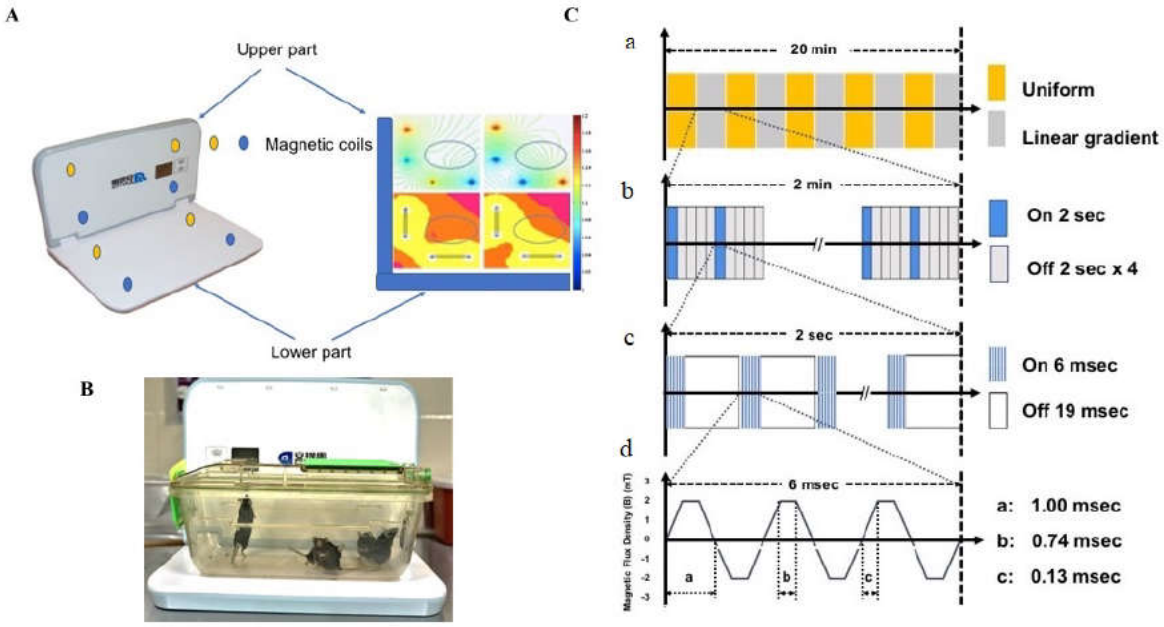

Figure 1. (A) Picture representing the LFMS device with magnetic field distribution, magnetic coils circled with yellow and blue colour presented in all four corners horizontally and vertically that generates intermittent magnetic field; the current density was represented on the right side; (B) LFMS machine with animals in their home cage, which received non-invasive extremely low field magnetic stimulation; (C) A schematic diagram representing the operational principle of LFMS device, a. every 2 min the magnetic field is switched between uniform (magnetic flux density) and linear gradient distribution. b. Magnetic pulses. Every 2 s output is followed by 8 s resting interval. c. In each 2 s, stimulation is composed of rhythmical trains spiking 6 ms pulses with intervals of 19 ms and constitutes the intermittent gamma burst stimulation at 40 Hz rhythm. d. Magnetic flux density.

At the end of the treatment period (48 h after the last MPTP injection), the mice were assessed for motor functions using beam walk and rotarod tests. Open field locomotor and stride length were measured, on the next day. Following motor function tests (on day 8), 11 mice/group were sacrificed by cervical dislocation under deep anesthesia (5% isoflurane; the depth of anesthesia confirmed by the observation of deep and shallow breathing and loss of withdrawal reflexes) and brain were isolated for dopamine measurement and western blotting. The remaining mice were perfused and brains were collected in 4% paraformaldehyde for immunohistochemistry [54].

4.4. Motor functional analysis

4.4.1. Beam walk test

Beam walk test was performed according to Sathiya et al. [52] with minor modification. Mice were pre-trained to traverse a narrow beam of 100 cm length to reach an enclosed escape platform. A bright light (approximately 60 W) was placed above the narrow beam to create an aversive stimulus. This encourages the mice to traverse the beam to the dark enclosed goal box. Following the treatment, mice were placed individually at the start of the beam and analyzed for the time taken to run over the beam, and the immobility period. The immobility period is the total time of all rests while traversing the beam. The maximum time given for a mouse to traverse the beam was 60 s and if the mouse did not reach the goal box in 60 s, the time taken was recorded as 60 s. The beam was cleaned with 70% alcohol between each animal. The observer who scored the test was masked to the treatment groups.

 doi:10.20944/preprints202305.0214.v1

4.4.2. Stride length

Stride length was measured according to Fernagut et al. [55] method. Apparatus consisted of a runway 4.5 (w) × 40 (l) × 9.5 (h) and a dark goal box 20 (w) ×14.5 (l) ×6.5 (h) placed at one end of the runway. The box had a hole (45 mm in diameter) facing the runway. The runway was illuminated by a halogen lamp (approximately 60 W), so that mice placed on the runway would run toward the box. The fore- and hind- paws of the mice were wetted with non-toxic colored ink and placed at the other end of the runway, which was covered with a strip of white paper. The time taken by the mice to cross the runway was recorded and the stride length for both the limbs were calculated as the distance between two fore paw prints (average of 3 consecutive readings) and a distance between two hind paw prints (average of 3 consecutive readings). The apparatus was cleaned with 70% alcohol between each animal. The observer who scored the behavior was masked to the treatment groups.

4.4.3. Rotarod

Rotarod test was performed according to Deacon's method [56] with a slight modification. The five-chambered rotarod machine (Series 8; IITC Life Science) was used for the experiment. Following the treatment, mice were placed on the rod, one in each chamber facing away from the direction of rotation. The rotation was started with the acceleration rate of 4 rpm/s. The time taken by the mice on the rotating rod was recorded. The test was repeated three times and the mean value for each animal was calculated. The maximum time and speed of the rotation was set as 120 s and 50 rpm, respectively. The apparatus was cleaned with 70% alcohol between each trial and the observer who scored the experiment was masked to the treatment groups.

4.4.4. Open field test

Locomotor activity was evaluated by placing the mouse into one corner of the open-field arena (40x40x30 cm; floor of the open field divided to 16 equal squares) and observed for 5 min. The total distance travelled, immobility period(s), number of total squares and center squares crossed were recorded. The floor of the maze was cleaned with 70% alcohol between each animal and the observer who scored the behavior was masked to the treatment groups [57].

4.5. Western blotting

SNpc and ST regions [58] were isolated (n=6) from the fresh brain and flash frozen in the liquid nitrogen. The tissues were then homogenized using lysis buffer (25 mM Tris, 150 mM NaCl, 0.1% sodium dodecyl sulphate, 0.5% sodium deoxycholate and 1% Triton X-100, pH 7–8 with protease inhibitors: 1 mm PMSF, 10 µg/µl aprotinin, 10 µg/ml pepstatin A, 10 µg/ml leupeptin, 2 mm Na3VO4, 20 mm sodium pyrophosphate, 3 mm benzamidine hydrochloride, and 4 mm glycerol 2-phosphate). The supernatant containing total protein was determined by using the Bradford Assay with the DC Protein assay dye (#5000111, Bio-Rad), boiled at 95°C with 2X sample loading buffer (#1610737, Bio-Rad) for 5 min. The samples (40 µg of protein concentration) were then loaded and separated using sodium dodecyl sulfate polyacrylamide gel electrophoresis (SDS-PAGE) and transferred onto polyvinyl difluoride (PVDF) membranes. The membranes were blocked with 5% fat-free milk for 1 hour at room temperature to block non-specific binding. The membranes were then washed with TBST (Tris-buffered saline, 0.1% Tween 20) 3 times, 5 min each. The target proteins were immunoblotted with primary antibodies (rabbit anti-TH [1:200; Cat# ab6211; RRID: AB_2240393; Abcam], mouse anti-NeuN [1:500; Cat# MAB377; RRID: AB_2298772; Millipore], mouse anti-GFAP [1:1000; Cat# MA5-12023; RRID: AB_10984338; Invitrogen], rabbit anti-IBA1 [1:1000; Cat# MA5-36257; RRID: AB_2890455; Invitrogen] and rabbit anti-Caspase 3 [1:1000; Cat# 9662S; RRID: AB_331439; Cell Signaling]) overnight at 4°C and then with corresponding HRP-conjugated secondary antibodies (goat anti-mouse IgG (Cat# 7076S; RRID: AB_330924) and goat anti-rabbit IgG (Cat# 7074S; RRID: AB_2099233) HRP linked; Cell Signaling). Mouse Anti-ß actin (C4) HRP [1:5000; Cat# sc-47778 HRP; RRID: AB_2714189; Santa Cruz Biotechnology] was used as the loading control and was incubated for 1 h at room temperature. The membranes were washed with TBST and exposed to enhanced

Preprints (www.preprints.org) | NOT PEER-REVIEWED | Posted: 4 May 2023 doi:10.20944/preprints202305.0214.v1

chemiluminescence reagent (Bio-Rad) and then imaged using ChemiDoc™ MP Imaging System. Protein bands of interest were analyzed using NIH ImageJ software and expressed as the ratio of target protein to β-actin [27].

4.6. Immunohistochemistry

Immunohistochemical evaluation of TH, NeuN and GFAP expression in SNpc and ST regions (n=6 from control and LFMS groups, and 7 from MPTP and MPTP+LFMS groups) were investigated using Bachman method [59] with a slight modification. The perfused brains were collected and stored at 4ºC for 2-3 days in 4% paraformaldehyde. 30-40 µm-thick sections through matched coronal levels of SNpc (sections approximately at Bregma -3.16 mm, interaural 0.64 mm region) and ST (sections approximately at Bregma 0.98 mm, interaural 4.78 mm region) were cut using vibratome and stored in cryoprotectant (25% glycerol, 30% ethylene glycol, 0.1% sodium azide and 1X PBS) at 4ºC until use. Four sections/regions/brains were selected in a random manner. The sections were incubated with 0.3% hydrogen peroxide to remove endogenous peroxidase interference. The non-specific binding was blocked with 5% BSA for 1 h and then the sections were incubated with biotinylated primary antibodies (rabbit anti-TH [1:100; Cat# ab6211; RRID: AB_2240393; Abcam], mouse anti-NeuN [1:100; Cat# MAB377; RRID: AB_2298772; Millipore] and mouse anti-GFAP [1:250; Cat# MA5-12023; RRID: AB_10984338; Invitrogen]) overnight. Next day, the sections were washed and incubated with secondary antibodies (goat biotinylated anti-mouse IgG [H&L; 1:500; Cat# BA-9200; RRID: AB_2336171] and goat biotinylated anti-rabbit IgG [H&L; 1:500; Cat# BA-1000; RRID: AB_2313606]; Vector Labs) for a period of 1 h. Phosphate buffered saline was used for washing between each step. The sections were stained with avidin-biotin substrate (VECTASTAIN® Elite ABC-HRP Kit, Peroxidase; Cat# PK-6100; RRID: AB_2336819) and then with 0.05% DAB solution. All sections were mounted and counterstained with Mayer's hematoxylin, and visualized in a phase contrast trinocular compound microscope (OMAX Microscopes, Canada; Software: Toupview version 3.7 (http://www.touptek.com/product/showproduct.php?id=103&lang=en, RRID: SCR_017998, ToupTek Photonics Co., Ltd., China) at 10X magnification.

Quantification of TH, NeuN and GFAP immunopositive cells in each section (Six animals per group; 4 non consecutive sections per animal, one section of every six was collected and used for each staining) were performed using NIH image J software (https://imagej.net/, RRID:SCR_003070). The number of immunopositive cells per mm^2 was counted at 100X magnification and the percentage of immunostaining of the target protein was calculated. The counting was performed randomly in 10 regions of the entire SNpc and ST regions and the mean value was calculated for each section. For TH in ST region, the intensity of colour developed was measured and the percentage of immunostaining with that of control was expressed. The person who performed immunostaining and scoring was masked to the treatment groups.

4.7. Enzyme-Linked Immunosorbent Assay (ELISA)

Experimental mice (n=5) were euthanized by cervical dislocation under deep anesthesia and the ST region was isolated from each brain. ST regions were processed for dopamine measurement using ELISA kit (Reddot Biotech Inc., Canada), following manufacturer's instructions. The homogenate for analysis was prepared using lysis buffer (25 mM Tris, 150 mM NaCl, 0.1% sodium dodecyl sulphate, 0.5% sodium deoxycholate, 1% Triton X-100, pH 7–8 and protease inhibitors). The intensity of colour developed was measured at 450 nm and is inversely proportional to the dopamine concentration. The minimum detectable level of dopamine using this kit was found to be less than 7.6 pg/ml. Various studies have measured dopamine level using HPLC technique. However, we measured dopamine level in the ST region using ELISA as this method is found to be precise and accurate, Nichkova et al. [60] validated ELISA for the measurement of dopamine content in urine samples.

4.8. Statistical analysis

Data were expressed individually and were tested for the normality of distribution using the Shapiro-Wilk test. Differences between the groups were analyzed using GraphPad Prism (version

 doi:10.20944/preprints202305.0214.v1

7.0, http://www.graphpad.com/, RRID:SCR_002798). A *P* value of less than 0.05 was considered statistically significant. All the data were tested for normality of distribution using Shapiro-Wilk test. The differences between groups were analyzed using either one-way ANOVA (for behavioral outcome, and dopamine data), or two-way ANOVA (for TH, NeuN, GFAP, IBA1, and caspase 3 data) followed by Tukey's multiple comparison as post hoc with SNpc and ST as factors. NIH image J software was used to analyse the protein bands of interest in western blot and the percentage of immunoreactivity in immunohistochemistry images. ANY-maze software was used to measure the total distance travelled in an open field test.

Acknowledgement: Authors thank the Saskatchewan Health Research Foundation (SHRF) for providing post-doctoral fellowship to SS and Collaborative Innovation Development (CID) grant to CT. Authors also thank Dr. Erin Kulhawy (University of Saskatchewan) for assisting with English editing and Dr. Mahshid Atapour (a faculty member in the Department of Mathematics and Statistics, Capilano University, Vancouver, Canada) for assisting with statistical analysis of the manuscript.

Conflict of Interest: Authors declare no conflict of Interest.

References

1. de Lau, L. M.; Breteler, M. M. Epidemiology of Parkinson's disease. *The Lancet Neurology* **2006**, 5, 525-535.
2. Balestrino, R.; Schapira, A. H. V. Parkinson disease. *European Journal of Neurology* **2020**, 27, 27-42.
3. Kalia, L. V.; Lang, A. E. Parkinson disease in 2015: Evolving basic, pathological and clinical concepts in PD. *Nature Reviews Neurology* **2016**, 12, 65-66.
4. Marino, B. L. B.; de Souza, L. R.; Sousa, K. P. A.; Ferreira, J. V.; Padilha, E. C.; da Silva, C. H. T. P.; Taft, C. A.; Hage-Melim, L. I. S. Parkinson's disease: A Review from the Pathophysiology to Diagnosis, New Perspectives for Pharmacological Treatment. *Mini-Reviews in Medicinal Chemistry* **2019**, 20, 754-767.
5. Simon, D. K.; Tanner, C. M.; Brundin, P. Parkinson Disease Epidemiology, Pathology, Genetics, and Pathophysiology. *Clinics in Geriatric Medicine* **2020**, 36, 1-12.
6. Korshunov, K. S.; Blakemore, L. J.; Trombley, P. Q. Dopamine: A Modulator of Circadian Rhythms in the Central Nervous System. *Frontiers in Cellular Neuroscience* **2017**, 11, 91.
7. Rascol, O.; Payoux, P.; Ory, F.; Ferreira, J. J.; Brefel-Courbon.; Montastruc, J. Limitations of current Parkinson's disease therapy. *Annals of Neurology* **2003,** 53, S3-12.
8. Rossi, S.; Hallett, M.; Rossini, P. M.; Pascual-Leone, A.; Safety of, T. M. S. C. G. Safety, ethical considerations, and application guidelines for the use of transcranial magnetic stimulation in clinical practice and research. *Clinical Neurophysiology* **2009**, 120, 2008-2039.
9. Chung, C. L.; Mak, M. K. Effect of Repetitive Transcranial Magnetic Stimulation on Physical Function and Motor Signs in Parkinson's Disease: A Systematic Review and Meta-Analysis. *Brain Stimulation* **2016**, 9, 475-487.
10. Hai-Jiao, W.; Ge, T.; Li-Na, Z.; Deng, C.; Da, X.; Shan-Shan, C.; Liu, L. The efficacy of repetitive transcranial magnetic stimulation for Parkinson disease patients with depression. *International Journal of Neuroscience* **2020**, 130, 19-27.
11. Lefaucheur, J. P.; Aleman, A.; Baeken, C.; Benninger, D. H.; Brunelin, J.; Di Lazzaro, V.; Filipović, S. R.; Grefkes, C.; Hasan, A.; Hummel, F. C.; et al. Evidence-based guidelines on the therapeutic use of repetitive transcranial magnetic stimulation (rTMS): An update (2014-2018). *Clinical Neurophysiology* **2020** 131, 474-528.

12. Dinkelbach, L.; Brambilla, M.; Manenti, R.; Brem, A. K. Non-invasive brain stimulation in Parkinson's disease: Exploiting crossroads of cognition and mood. *Neuroscience & Biobehavioral Reviews* **2017**, 75, 407-418.
13. Goodwill, A. M.; Lum, J. A. G.; Hendy, A. M.; Muthalib, M.; Johnson, L.; Albein-Urios, N.; Teo, W. Using non-invasive transcranial stimulation to improve motor and cognitive function in Parkinson's disease: a systematic review and meta-analysis. *Scientific Reports* **2017**, 7, 14840.
14. Rektorova, I.; Anderkova, L. Noninvasive Brain Stimulation and Implications for Nonmotor Symptoms in Parkinson's Disease. *International Review of Neurobiology* **2017**, 134, 1091-1110.
15. Malling, A. S. B.; Morberg, B. M.; Wermuth, L.; Gredal, O.; Bech, P.; Jensen, B. R. Effect of transcranial pulsed electromagnetic fields (T-PEMF) on functional rate of force development and movement speed in persons with Parkinson's disease: A randomized clinical trial. *PLoS One* **2018**, 13, e0204478.
16. Manenti, R.; Cotelli, M. S.; Cobelli, C.; Gobbi, E.; Brambilla, M.; Rusich, D.; Alberici, A.; Padovani, A.; Borroni, B.; Cotelli, M. Transcranial direct current stimulation combined with cognitive training for the treatment of Parkinson Disease: A randomized, placebo-controlled study. *Brain Stimulation* **2018**, 11, 1251-1262.
17. Woods, A. J.; Antal, A.; Bikson, M.; Boggio, P. S.; Brunoni, A. R.; Celnik, P.; Cohen, L. G.; Fregni, F.; Herrmann, C. S.; Kappenman, E. S.; et al. A technical guide to tDCS, and related non-invasive brain stimulation tools. *Clinical Neurophysiology* **2016**, 127, 1031-1048.
18. Martiny, K.; Lunde, M.; Bech, P. Transcranial low voltage pulsed electromagnetic fields in patients with treatment-resistant depression. *Biological Psychiatry* **2010**, 68, 163-169.
19. Rohan, M.; Parow, A.; Stoll, A. L.; Demopulos, C.; Friedman, S.; Dager, S.; Hennen, J.; Cohen, B. M.; Renshaw P. F. Low-field magnetic stimulation in bipolar depression using an MRI-based stimulator. *American Journal of Psychiatry* **2004**, 161, 93-98.
20. Shafi, M.; Stern, A. P.; Pascual-Leone, A. Adding low-field magnetic stimulation to noninvasive electromagnetic neuromodulatory therapies. *Biological Psychiatry* **2014**, 76, 170-171.
21. Jin, Y.,; Phillips, B. A pilot study of the use of EEG-based synchronized Transcranial Magnetic Stimulation (sTMS) for treatment of Major Depression. *BMC Psychiatry* **2014**, 14, 13.
22. Leuchter, A. F.; Cook, I, A.; Feifel, D.; Goethe, J. W.; Husain, M.; Carpenter, L. L.; Thase, M. E.; Krystal, A. D.; Philip, N. S.; Bhati, M. T.; et al. Efficacy and Safety of Low-field Synchronized Transcranial Magnetic Stimulation (sTMS) for Treatment of Major Depression. *Brain Stimulation* **2015**, 8, 787-794.
23. Rohan, M. L.; Yamamoto, R. T.; Ravichandran, C. T.; Cayetano, K. R.; Morales, O. G.; Olson, D. P.; Vitaliano, G.; Paul, S. M.; Cohen, B. M. Rapid mood-elevating effects of low field magnetic stimulation in depression. *Biological Psychiatry* **2014**, 76, 186-193.
24. Straaso, B.; Lauritzen, L.; Lunde, M.; Vinberg, M.; Lindberg, L.; Larsen, E. R.; Dissing, S.; Bech, P. Dose-remission of pulsating electromagnetic fields as augmentation in therapy-resistant depression: a randomized, double-blind controlled study. *Acta Neuropsychiatrica* **2014**, 26, 272-279.
25. Dong, Q.; Wang, Y.; Gu, P.; Shao, R.; Zhao, L.; Liu, X.; Wang, Z.; Wang, M. The Neuroprotective Mechanism of Low-Frequency rTMS on Nigral Dopaminergic Neurons of Parkinson's Disease Model Mice. *Parkinson's Disease* **2015**, 2015, 564095.
26. Zhang, Z. C.; Luan, F.; Xie, C.; Geng, D.; Wang, Y.; Ma, J. Low-frequency transcranial magnetic stimulation is beneficial for enhancing synaptic plasticity in the aging brain. *Neural Regeneration Research* **2015**, 10, 916-924.
27. Sekar, S.; Zhang, Y.; Miranzadeh Mahabadi, H.; Parvizi, A.; Taghibiglou, C. Low-Field Magnetic Stimulation Restores Cognitive and Motor Functions in the Mouse Model of Repeated Traumatic Brain Injury: Role of Cellular Prion Protein. *Journal of Neurotrauma* **2019**, 36, 3103-3114.
28. Mooshekhian, A.; Sandhini, T.; Wei, Z.; Van Bruggen, R.; Li, H.; Li, X.; Zhang, Y. Low-field magnetic stimulation improved cuprizone-induced depression-like symptoms and demylination in female mice. *Experimental and Therapeutic Medicine* **2022**, 23, 210.
29. Wang, Z.; Baharani, A.; Truong, D.; Bi, X.; Wang, F.; Li, X.; Verge, V. M. K.; Zhang, Y. Low field magnetic stimulation promotes myelin repair and cognitive recovery in chronic cuprizone mouse model. *Clinical and Experimental Pharmacology and Physiology* **2021**, 48, 1090-1102.
30. Jia, X.; Kohn, A. Gamma rhythms in the brain. *PLoS Biology* **2011**, 9, e1001045.
31. Uhlhaas, P. J.; Singer, W. Neural synchrony in brain disorders: relevance for cognitive dysfunctions and pathophysiology. *Neuron* **2006**, 52, 155-168.

32. Nowak, M.; Zich, C.; Stagg, C. J. Motor Cortical Gamma Oscillations: What Have We Learnt and Where Are We Headed? *Current Behavioral Neuroscience Reports* **2018**, 5, 136-142.
33. Chartove, J. A. K.; McCarthy, M. M.; Pittman-Polletta, B. R.; Kopell, N. J. A biophysical model of striatal microcircuits suggests gamma and beta oscillations interleaved at delta/theta frequencies mediate periodicity in motor control. *PLOS Computational Biology* **2020**, 16, e1007300.
34. Sulzer, D. Multiple hit hypotheses for dopamine neuron loss in Parkinson's disease. *Trends in Neurosciences* **2007**, 30, 244-250.
35. Adams, J. D.; Jr., Chang, M. L.; Klaidman, L. Parkinson's disease--redox mechanisms. *Current Medicinal Chemistry* **2001**, 8, 809-814.
36. Lofredi, R.; Neumann, W.; Bock, A.; Horn, A.; Huebl, J.; Siegert, S.; Schneider, G.; Krauss, J. K.; Kühn A. A. Dopamine-dependent scaling of subthalamic gamma bursts with movement velocity in patients with Parkinson's disease. *Elife* **2018**, 7, e31895.
37. Tabrez, S.; Jabir, N. R.; Shakil, S.; Greig, N. H.; Alam, Q.; Abuzenadah, A. M.; Damanhouri, G. A.; Kamal, M. A. A synopsis on the role of tyrosine hydroxylase in Parkinson's disease. *CNS & Neurological Disorders - Drug Targets* **2012**, 11, 395-409.
38. Gebreyesus, H. H.; Gebremichael, T. G. The Potential Role of Astrocytes in Parkinson's Disease (PD). *Medical Sciences (Basel)* **2020**, 8, 7.
39. Udovin, L.; Quarracino, C.; Herrera, M. I.; Capani, F.; Otero-Losada, M.; Perez-Lloret, S. Role of Astrocytic Dysfunction in the Pathogenesis of Parkinson's Disease Animal Models from a Molecular Signaling Perspective. *Neural Plasticity* **2020**, 2020, 1859431.
40. Haque, M. E.; Akther, M.; Jakaria, M.; Kim, I.; Azam, S.; Choi, D. Targeting the microglial NLRP3 inflammasome and its role in Parkinson's disease. *Movement Disorders* **2020**, 35, 20-33.
41. Lazdon, E.; Stolero, N.; Frenkel, D. Microglia and Parkinson's disease: footprints to pathology. *Journal of Neural Transmission (Vienna)* **2020**, 127, 149-158.
42. Bachiller, S.; Jiménez-Ferrer, I.; Paulus, A.; Yang, Y.; Swanberg, M.; Deierborg, T.; Boza-Serrano, A. Microglia in Neurological Diseases: A Road Map to Brain-Disease Dependent-Inflammatory Response. *Frontiers in Cellular Neuroscience* **2018**, 12, 488.
43. Sofroniew, M. V. Astrogliosis. *Cold Spring Harbor Perspectives in Biology* **2014**, 7, a020420.
44. Cheyne, D.; Ferrari, P. MEG studies of motor cortex gamma oscillations: evidence for a gamma "fingerprint" in the brain? *Frontiers in Human Neuroscience* **2013**, 7, 575.
45. Fricke, C.; Duesmann, C.; Woost, T. B.; Hofen-Hohloch, J. V.; Rumpf, J.; Weise, D.; Classen, J. Dual-Site Transcranial Magnetic Stimulation for the Treatment of Parkinson's Disease. *Frontiers in Neurology* **2019**, 10, 174.
46. Yang, C.; Guo, Z.; Peng, H.; Xing, G.; Chen, H.; McClure, M. A.; He, B.; He, L.; Du, F.; Xiong, L.; et al. Repetitive transcranial magnetic stimulation therapy for motor recovery in Parkinson's disease: A Meta-analysis. *Brain and Behavior* **2018**, 8, e01132.
47. Matsumoto, H.; Ugawa, Y. Repetitive Transcranial Magnetic Stimulation for Parkinson's Disease: A Review. *Brain and Nerve* **2017**, 69, 219-225.
48. Hanajima, R.; Terao, Y.; Shirota, Y.; Ohminami, S.; Tsutsumi, R.; Shimizu, T.; Tanaka, N.; Okabe, S.; Tsuji, S.; Ugawa, Y. Triad-conditioning transcranial magnetic stimulation in Parkinson's disease. *Brain Stimulation* **2014**, 7, 74-79.
49. Chervyakov, A. V.; Chernyavsky, A. Y.; Sinitsyn, D. O.; Piradov, M. A. Possible Mechanisms Underlying the Therapeutic Effects of Transcranial Magnetic Stimulation. *Frontiers in Human Neuroscience* **2015**, 9, 303.
50. Morberg, B. M.; Malling, A. S.; Jensen, B. R.; Gredal, O.; Bech , P.; Wermuth, L. Parkinson's disease and transcranial pulsed electromagnetic fields: A randomized clinical trial. *Movement Disorders* **2017**, 32, 625-626.
51. Huang, D.; Xu, J.; Wang, J.; Tong, J.; Bai, X.; Li, H.; Wang, Z.; Huang, Y.; Wu, Y.; Yu, M.; et al. Dynamic Changes in the Nigrostriatal Pathway in the MPTP Mouse Model of Parkinson's Disease. *Parkinson's Disease* **2017**, 2017, 9349487.
52. Sathiya, S.; Ranju, V.; Kalaivani, P.; Priya, R. J.; Sumathy, H.; Sunil, A. G.; Babu, C. S. Telmisartan attenuates MPTP induced dopaminergic degeneration and motor dysfunction through regulation of alpha-synuclein and neurotrophic factors (BDNF and GDNF) expression in C57BL/6J mice. *Neuropharmacology* **2013**, 73, 98-110.
53. Zhen, J.; Qian, Y.; Weng, X.; Su, W.; Zhang, J.; Cai, L.; Dong, L.; An, H.; Su, R.; Wang, J.; et al. Gamma rhythm low field magnetic stimulation alleviates neuropathologic changes and rescues memory and

 doi:10.20944/preprints202305.0214.v1

cognitive impairments in a mouse model of Alzheimer's disease. *Alzheimer's & dementia (New York)* **2017,** 3, 487-497.

54. Zhang, Y.; Schlussman, S. D.; Rabkin, J.; Butelman, E. R.; Ho, A.; Kreek, M. J. Chronic escalating cocaine exposure, abstinence/withdrawal, and chronic re-exposure: effects on striatal dopamine and opioid systems in C57BL/6J mice. *Neuropharmacology* **2013**, 67, 259-266.
55. Fernagut, P. O.; Diguet, E.; Labattu, B.; Tison, F. A simple method to measure stride length as an index of nigrostriatal dysfunction in mice. *Journal of Neuroscience Methods* **2002**, 113, 123-130.
56. Deacon, R. M. Measuring motor coordination in mice. *Journal of Visualized Experiments* **2013**, 75, e2609.
57. Salas, R.; Pieri, F.; Fung, B.; Dani, J. A.; De Biasi, M. Altered anxiety-related responses in mutant mice lacking the beta4 subunit of the nicotinic receptor. *Journal of Neuroscience* **2003**, 23, 6255-6263.
58. Paxinos, G.; Franklin, K. The Mouse Brain in Stereotaxic Coordinates. Second edn, Academic Press **2001**.
59. Bachman, J. Immunohistochemistry on freely floating fixed tissue sections. *Methods in Enzymology* **2013**, 533, 207-215.
60. Nichkova, M.; Wynveen, P. M.; Marc, D. T.; Huisman, H.; Kellermann, G. H. Validation of an ELISA for urinary dopamine: applications in monitoring treatment of dopamine-related disorders. *Journal of Neurochemistry* **2013**, 125, 724-735.